Dorsolateral prefrontal cortex supports speech perception in listeners with cochlear implants

Arefeh Sherafati[1], Noel Dwyer[2], Aahana Bajracharya[2], Mahlega S. Hassanpour[3], Adam T. Eggebrecht[1], Jill B. Firszt[2], Joseph P. Culver[1, 4, 5, 6], Jonathan E. Peelle[2*]

[1] Department of Radiology, Washington University in St. Louis, St. Louis, MO, USA

[2] Department of Otolaryngology, Washington University in St. Louis, St. Louis, MO, USA

[3] Moran Eye Center, University of Utah, Salt Lake City, UT, USA

[4] Department of Physics, Washington University in St. Louis, St. Louis, MO, USA

[5] Department of Biomedical Engineering, Washington University in St. Louis, St. Louis, MO, USA

[6] Division of Biology and Biomedical Sciences, Washington University in St. Louis, St. Louis, MO, USA

[*]jpeelle@wustl.edu

Abstract

Cochlear implants are neuroprosthetic devices that can restore hearing in individuals with severe to profound hearing loss by electrically stimulating the auditory nerve. Because of physical limitations on the precision of this stimulation, the acoustic information delivered by a cochlear implant does not convey the same level of spectral detail as that conveyed by normal hearing. As a result, speech understanding in listeners with cochlear implants is typically poorer and more effortful than in listeners with normal hearing. The brain networks supporting speech understanding in listeners with cochlear implants are not well understood, partly due to difficulties obtaining functional neuroimaging data in this population. In the current study, we assessed the brain regions supporting spoken word understanding in adult listeners with right unilateral cochlear implants (n=20) and matched controls (n=18) using high-density diffuse optical tomography (HD-DOT), a quiet and non-invasive imaging modality with spatial resolution comparable to that of functional MRI. We found that while listening to spoken words in quiet, listeners with cochlear implants showed greater activity in the left dorsolateral prefrontal cortex, overlapping with functionally-defined domain-general processing seen in a spatial working memory task. These results suggest that listeners with cochlear implants require greater cognitive processing during speech understanding than listeners with normal hearing, supported by compensatory recruitment in the left dorsolateral prefrontal cortex.

Introduction

Cochlear implants (CIs) are neuroprosthetic devices that can restore hearing in individuals with severe to profound hearing loss by electrically stimulating the auditory nerve. Because of physical limitations on the precision of this stimulation—including, for example, the spatial spread of electrical current (Garcia, Goehring et al. 2021)—the auditory stimulation delivered by a CI does not convey the same level of spectral detail as normal hearing. As a result, speech understanding in listeners with CIs is poorer than in listeners with normal hearing (Firszt, Holden et al. 2004). Notably, even in quiet, listeners with CIs report increased effort during listening (Dwyer, Firszt et al. 2014). In spite of these challenges, many listeners with CIs attain significant levels of auditory speech understanding. This remarkable success raises the question of how listeners with CIs make sense of a degraded acoustic signal.

One area of key importance is understanding the degree to which listeners with CIs rely on nonlinguistic cognitive mechanisms to compensate for a degraded acoustic signal. In listeners with normal hearing, cognitive demands are increased when speech is acoustically challenging (Peelle 2018). For example, even when speech is completely intelligible, acoustically-degraded speech is more difficult to remember than acoustically clear speech (Rabbitt 1968, Cousins, Dar et al. 2014, Ward, Rogers et al. 2016, Koeritzer, Rogers et al. 2018). These findings suggest that to understand acoustically challenging speech, listeners need to engage domain-general cognitive resources. In a limited-capacity cognitive system (Wingfield 2016), such recruitment necessarily reduces the resources available for other tasks, such as memory encoding.

Cognitive demands during speech understanding are supported by several brain networks that supplement classic frontotemporal language networks. The cingulo-opercular network, for example, is engaged during particularly challenging speech (Eckert, Menon et al. 2009, Vaden, Teubner-Rhodes et al. 2017) and supports successful comprehension during difficult listening (Vaden, Kuchinsky et al. 2013). The activity in dorsolateral prefrontal cortex (DLPFC) complements the cingulo-opercular network and varies parametrically with speech intelligibility (Davis and Johnsrude 2003). Activity in DLPFC is associated with cognitive demands in a wide range of tasks (Duncan 2010), consistent with domain-general cognitive control (Braver 2012). However, the functional anatomy of DLPFC is also complex (Noyce, Cestero et al. 2017), and dissociating nearby language and domain-general processing regions is challenging (Fedorenko, Duncan et al. 2012).

Then, a central question concerns the degree to which listeners with CIs rely on cognitive processing outside core speech processing regions, such as DLPFC. Obtaining precise spatially-localized images of regional brain activity has been difficult in listeners with CIs, given that functional MRI is not possible (or subject to artifact) due to the CI hardware. Thus, optical brain imaging (Peelle 2017) has become a method of choice for studying functional activity in CI listeners (Lawler, Wiggins et al. 2015, Olds, Pollonini et al. 2016, Anderson, Wiggins et al. 2017, Lawrence, Wiggins et al. 2018, Zhou, Seghouane et al. 2018). In the current study, we use high-density diffuse optical tomography (HD-DOT) (Eggebrecht, Ferradal et al. 2014), previously validated in speech studies in listeners with normal hearing (Hassanpour, Eggebrecht et al. 2015, Hassanpour, Eggebrecht et al. 2017, Schroeder, Sherafati et al. 2020). HD-DOT provides high spatial resolution and homogenous sensitivity over the field of view that captures known speech-related brain regions (White and Culver 2010). We examine the brain regions supporting single word processing in listeners with a right unilateral CI relative to that in a group of matched controls. We hypothesized that listeners with CIs would exhibit greater recruitment in regions of DLPFC compared to normal hearing controls.

Methods

Data and code availability

Summary data and analysis scripts are available in https://osf.io/nkb5v/?view_only=2c8ef3af126542a49be055d50ac935d4.

Subjects

We recruited 21 adult CI patients and 19 age- and sex-matched controls (demographic information in **Table 1**). We excluded one CI user due to poor signal quality (evaluated as mean band limited SNR of all source-detectors) and one control due to excessive motion (see **Fig. S6**, and **supplementary materials** for details). All patients had a unilateral right CI and controls had normal bilateral hearing. All subjects were native speakers of English with no self-reported history of neurological or psychiatric disorders. All aspects of these studies were approved by the Human Research Protection Office of the Washington University School of Medicine. Subjects were recruited from the Washington University campus and the surrounding community (IRB 201101896, IRB 201709126). All subjects gave informed consent and were compensated for their participation in accordance with institutional and national guidelines.

Table 1: Demographic information.

Population	Control	CI users
Number of subjects (# of females)	18 (10)	20 (11)
Mean age at test in years (std)	56.05 (12.26)	56.80 (14.09)
Mean years of CI use (std)	NA	8.10 (6.51)
Mean speech perception score (AzBioSentences) (std), max = 1	0.99 (0.01)	0.88 (0.09)
Mean right ear 4fPTA* (std)	16.02 (6.74)	21.85 (5.30) with CI on
Mean left ear 4fPTA* (std)	16.61 (7.67)	91.25 (26.77) unaided
Mean left ear 4fPTA* at test[1] (std)	NA	73.28 (37.72)
Mean duration of deafness right ear	NA	12.58 (11.74)

*4fPTA, pure tone average at 4 frequencies, 500, 1000, 2000, 4000 Hz. If no response at a given frequency, a value of 120 dB HL was assigned.

[1] With hearing aid, if the subject used amplification. Eight out of twenty CI users had hearing aids.

HD-DOT system

Data were collected using a continuous-wave HD-DOT system comprised of 96 sources (LEDs, at both 750 and 850 nm) and 92 detectors (coupled to avalanche photodiodes, APDs, Hamamatsu C5460-01) to enable oxy and deoxyhemoglobin spectroscopy (**Fig. 1**) (Eggebrecht, Ferradal et al. 2014). The design of this HD-DOT system provides more than 1200 usable source-detector measurements at a 10 Hz full-field frame rate. This system has been validated for successfully mapping cortical responses to hierarchical language paradigms and naturalistic stimuli with comparable sensitivity and specificity to fMRI (Eggebrecht, Ferradal et al. 2014, Hassanpour, Eggebrecht et al. 2015, Fishell, Burns-Yocum et al. 2019).

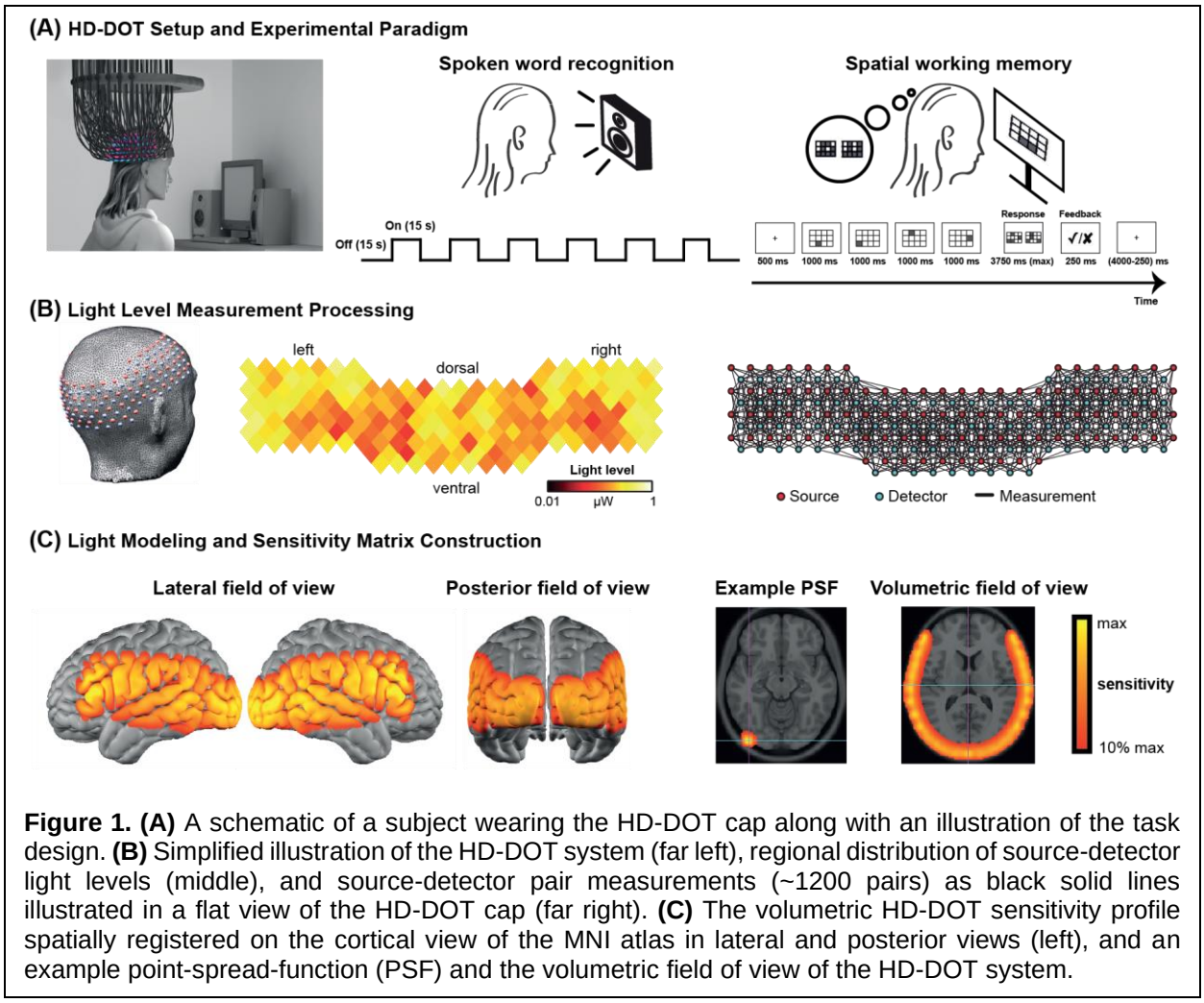

Figure 1. (A) A schematic of a subject wearing the HD-DOT cap along with an illustration of the task design. **(B)** Simplified illustration of the HD-DOT system (far left), regional distribution of source-detector light levels (middle), and source-detector pair measurements (~1200 pairs) as black solid lines illustrated in a flat view of the HD-DOT cap (far right). **(C)** The volumetric HD-DOT sensitivity profile spatially registered on the cortical view of the MNI atlas in lateral and posterior views (left), and an example point-spread-function (PSF) and the volumetric field of view of the HD-DOT system.

Experimental design

Subjects were seated on a comfortable chair in an acoustically isolated room facing an LCD screen located 76 cm from them, approximately at their eye level. The auditory stimuli were presented through two speakers located approximately 150 cm from the subjects' ears. Subjects were instructed to fixate on a white crosshair against a gray background while listening to the auditory stimuli, holding a keyboard on their lap for the stimuli that required their response (**Fig. 1A**, left panel). The HD-DOT cap was fitted to the subject's head to maximize optode-scalp coupling, assessed via real-time coupling coefficient readouts using an in-house software. The stimuli were presented using Psychophysics Toolbox 3 package (Brainard 1997) (RRID:SCR_002881) in MATLAB 2010b.

The spoken word recognition paradigm consisted of six blocks of spoken words per run. Each block contained 15 seconds of spoken words (one word per second), followed by 15 seconds of silence. Two runs were performed in each study session with a total of 180 words in about 6 minutes (**Fig. 1A**, middle panel).

Based on indications of DLPFC activity in our preliminary results, we adopted the spatial working memory task introduced in previous studies (Fedorenko, Behr et al. 2011, Fedorenko, Duncan et al. 2013) in the remaining subjects to aid in functionally localizing domain-general

regions of the prefrontal cortex. In this spatial working memory task, subjects were asked to remember four locations (easy condition) or eight locations (hard condition) in a 3×4 grid. Following each trial, subjects had to choose the pattern they saw among 2-choice grids, one with correct and one with incorrect locations. This task requires keeping sequences of elements in memory for a brief period and has been shown to activate DLPFC (**Fig. 1A**, right panel). Each run for the spatial working memory task was about 8 minutes, with a total of 48 trials in the run.

Data processing

HD-DOT data were pre-processed using the NeuroDOT toolbox (A. T. Eggebrecht 2019). Source-detector (SD) pair light level measurements were converted to log-ratio by calculating the temporal mean of a given SD-pair measurement as the baseline for that measurement. Noisy measurements were empirically defined as those that have greater than 7.5% temporal standard deviation in the least noisy (lowest mean motion) 60 seconds of each run (Eggebrecht, Ferradal et al. 2014, Sherafati, Snyder et al. 2020). Then, channels with greater than 33% noisy first or second nearest neighbor measurements (nn1 and nn2) were excluded (**Fig. S4**). The data were next high pass filtered at 0.02 Hz. The global superficial signal was estimated as the average of the nn1 measurements (13 mm SD-pair separation) and regressed from the data (Gregg, White et al. 2010). The optical density time-courses were then low pass filtered to 0.5 Hz to the physiological brain signal band and temporally downsampled from 10 Hz to 1 Hz. A wavelength-dependent forward model of light propagation was computed using the ICBM152 anatomical atlas using the non-uniform tissue structures: scalp, skull, CSF, gray matter, and white matter (Ferradal, Eggebrecht et al. 2014) (**Fig. 1C**). Relative changes in the concentrations of oxygenated, deoxygenated, and total hemoglobin (ΔHbO, HbR, ΔHbT) were obtained from the absorption coefficient changes by the spectral decomposition of the extinction coefficients of oxygenated and deoxygenated hemoglobin at the two wavelengths (750 nm and 850 nm). After inverting the sensitivity matrix, relative changes in absorption at the two wavelengths were reconstructed using Tikhonov regularization and spatially variant regularization (Eggebrecht, Ferradal et al. 2014). After post-processing, we resampled all data to the $3 \times 3 \times 3$ mm^3 MNI atlas using a linear affine transformation for group analysis. In addition to the standard HD-DOT pre-processing steps used in the NeuroDOT toolbox, we used a comprehensive data quality assessment pipeline (**Supplementary materials**) to exclude the data runs with low heartbeat SNR or high motion levels.

After pre-processing, the response for the speech task was estimated using a standard general linear model (GLM) framework. The design matrix was constructed using onsets and durations of the stimulus presentation convolved with a canonical hemodynamic response function (HRF). This HRF was created using a two-gamma function (2 s delay time, 7 s time to peak, and 17 s undershoot) fitted to the HD-DOT data described in a previous study (Hassanpour, Eggebrecht et al. 2015). We included both runs for each subject in one design matrix using custom MATLAB scripts (**Fig. S3A**).

For modeling the spatial working memory task, we used a standard GLM with two columns representing easy and hard conditions. The duration of each easy or hard trial was modeled as the total time of stimulus presentation and evaluation. Events were convolved with the same canonical HRF described in the spoken word perception task to model hemodynamic responses (Hassanpour, White et al. 2014). Due to the novelty of this task for CI users and an age-matched control group, we have used the easy + hard response maps as a reference for defining the DLPFC ROI (as opposed to the hard > easy previously used for younger populations).

After estimating the response (β map) for each subject for each task, we performed a second-level analysis in SPM12 (RRID:SCR_007037). Extracted time traces for each subject were then calculated using a finite impulse response model.

We only present the ΔHbO results in the main figures as we have found that the ΔHbO signal exhibits a higher contrast-to-noise ratio compared to ΔHbR or ΔHbT (Eggebrecht, Ferradal et al. 2014, Hassanpour, White et al. 2014).

Region of interest analysis

To perform a more focused comparison between controls and CI users, we objectively defined three regions of interest (ROIs), independent from our spoken word recognition dataset for statistical analysis.

We defined the left DLPFC ROI based on the response of the spatial working memory task in a group of subjects using the cluster of activation around the DLPFC region after $p < 0.05$ (uncorrected) voxelwise thresholding.

To define the left and right auditory ROIs, we used a previously published fMRI resting state dataset (Sherafati, Snyder et al. 2020) that was masked by the field of view of our HD-DOT system. We defined the left and right auditory ROIs by selecting a 5 mm radius seed in the contralateral hemisphere ([70.5, -24, 3], [-67.5, -27, 3]) and finding the Pearson correlation between the time-series of the seed region with all other voxels in the field of view. Correlation maps in individuals were Fisher's z-transformed and averaged across subjects. More details are provided in the results section.

Results

Multi-session single subject results

Due to the expected variability across CI users and difficulties in defining single subject ROIs, we performed a small multi-session study from one of our CI subjects for 6 sessions (**Fig. 2**). We collected 2 runs of spoken word perception per session (for 6 sessions) and 1 run of spatial working memory task per session (for 4 sessions). This multi-session analysis enabled localizing

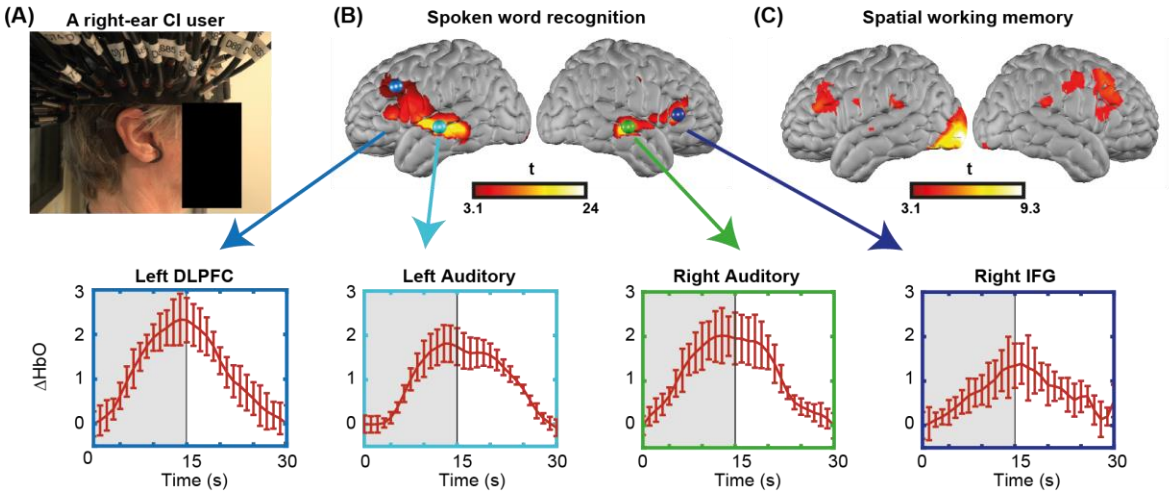

Figure 2 | Single subject data from one CI user across multiple sessions. (A) A CI user wearing the HD-DOT cap. **(B)** Response to the spoken words across 6 sessions (72 trials, each 15 sec stimuli, 15 sec rest). Hemodynamic response time-traces are plotted for peak activation values across 6 sessions for 4 key brain regions. The seed colors match the plot boundaries with error bars indicating the standard error of the mean. **(C)** Response to the spatial working memory task for the same right-ear CI user across 4 sessions (40 min of data).

the left and right DLPFC based on the non-verbal spatial working memory task for this subject (**Fig. 2C**). It also revealed the engagement of regions beyond the auditory cortex, including the DLPFC during the word perception task (**Fig. 2B**). Time-traces of oxyhemoglobin concentration change show a clear event-related response for four selected regions in the word perception results (**Fig. 2**).

Functionally defined ROIs

To accurately localize the elevated prefrontal cortex activation in the CI group, we collected HD-DOT data from 11 subjects (6 controls and 5 CI users in 15 sessions) using a spatial working memory task. This task robustly activates DLPFC due to its working memory demands (and visual cortex because of its visual aspect). We chose this task to better localize the DLPFC ROI for performing an ROI-based statistical analysis between controls and CI users. Our results show strong bilateral visual and DLPFC activations in response to this task (**Fig. 3A** left). We then defined the left DLPFC ROI as the cluster of activation in the left DLPFC region, as described in the methods section (**Fig.3A** right).

We defined the left and right auditory ROIs by selecting a seed in the opposite hemisphere (as described in the methods) and finding the Pearson correlation between the time-series of the seed region with all other voxels in the field of view. Correlation maps in individuals were Fisher's z-transformed and averaged across subjects (**Fig. 3B-C left**). Right/left auditory ROIs were defined by masking the correlation map to include only the right/left hemisphere (**Fig. 3B-C right**).

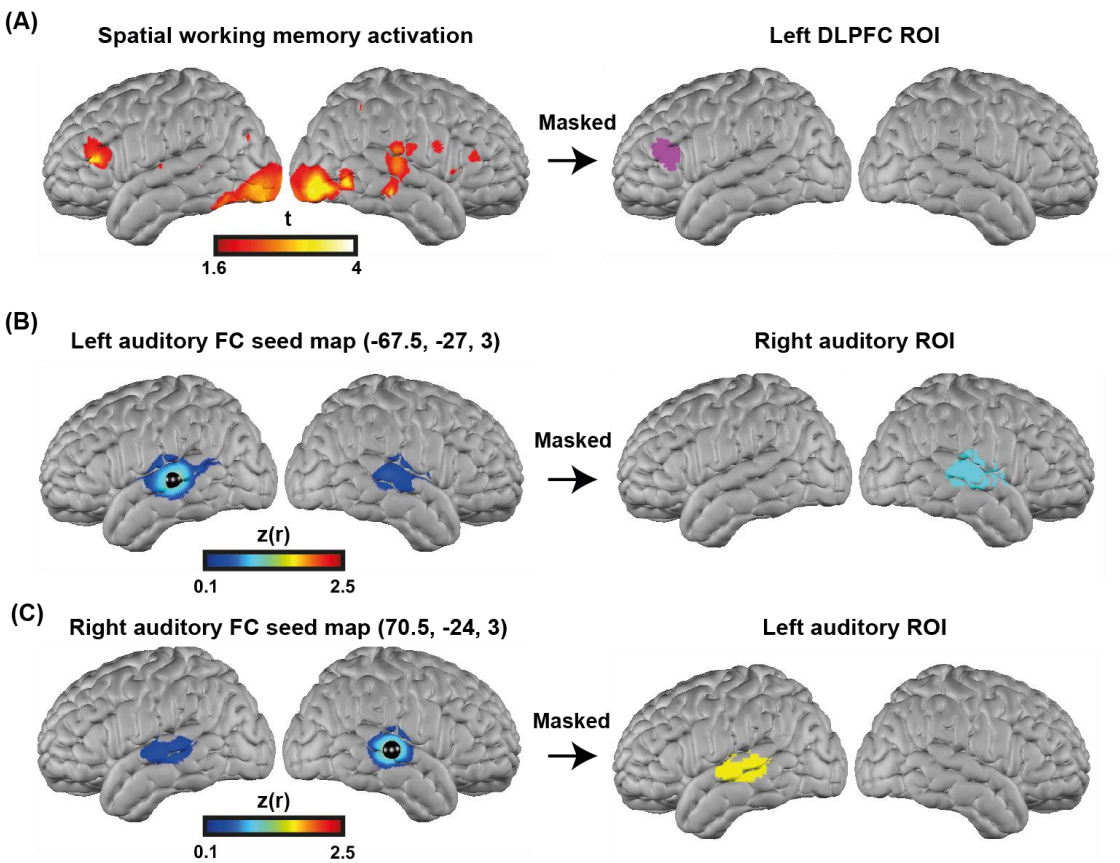

Figure 3 | Defining functional ROIs. (A) Spatial working memory activation for 5 CI users and 6 controls over 15 sessions. The DLPFC ROI was defined as the cluster of activation in the DLPFC region, survived after $p < 0.05$ (uncorrected) voxelwise thresholding. (**B)** Seed-based correlation map for a seed located in the left auditory cortex [-67.5, -27, 3] in MNI space (left map). Right auditory ROI defined by masking the correlation map to include only the right hemisphere (right map). (**C)** Seed-based correlation map for a seed located in the right auditory cortex [70.5, -24, 3] in MNI space (left map). Left auditory ROI defined by masking the correlation map to include only the left hemisphere (right map).

Mapping the brain response to spoken words

We first investigated the degree of auditory activation in both control and CI groups by assessing the activity in a block-design single word presentation task. We found strong bilateral superior temporal gyrus (STG) activations in controls similar to our previous studies using the same paradigm (Eggebrecht, Ferradal et al. 2014, Hassanpour, Eggebrecht et al. 2015), as well as a strong left STG and a smaller right STG activation for the CI users (**Fig. 4A-B**). In addition, we observed strong left-lateralized activations in regions beyond the auditory cortex, including parts of the prefrontal cortex in the CI user group (**Fig. 4B**). The temporal profile of the hemodynamic response in three selected ROIs also reflects the increased activity in the left DLPFC region in the CI users relative to controls, and a decrease in both left and right auditory cortical regions. Two sample t-statistics for the mean β values in each ROI support a statistically significant difference between the control and CI groups in left DLPFC and right auditory cortex (**Fig. 5D**).

246 **Figure S7** provides the β maps of oxyhemoglobin (HbO), deoxyhemoglobin (HbR), and total
247 hemoglobin (HbT) for controls (panel A), CI users (panel B), and CI greater than controls (panel
248 C).
249

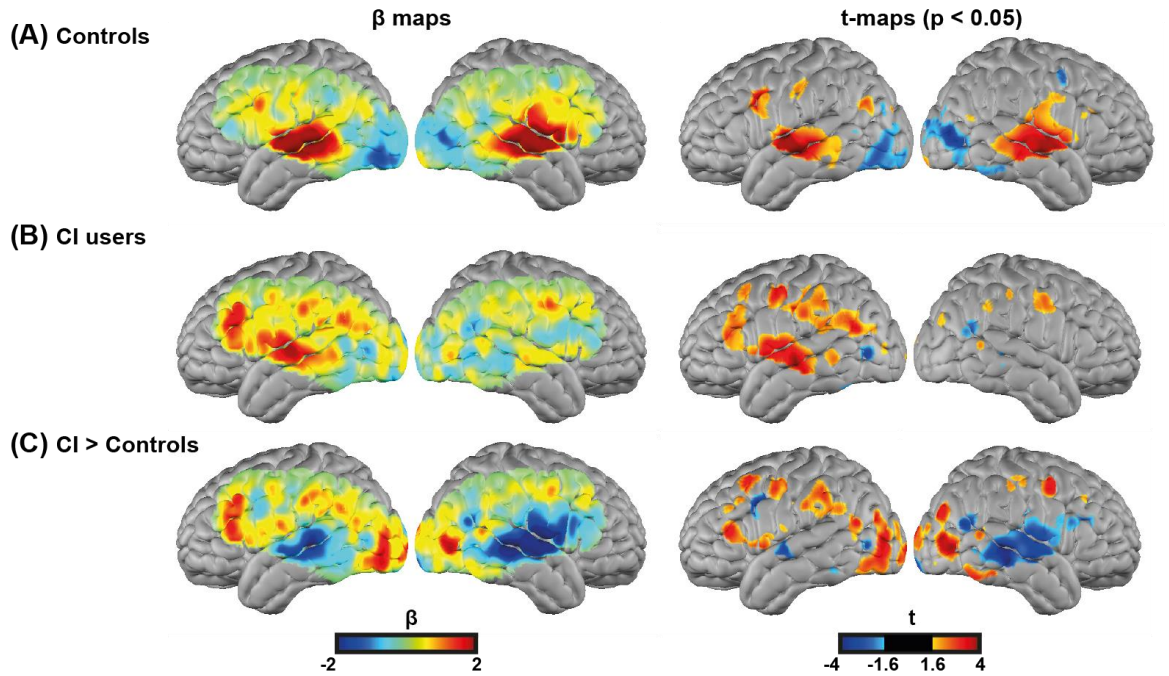

Figure 4 | Spoken word recognition group maps. Response to the spoken words in **(A)** 18 controls and **(B)** 20 right-ear CI users. **(C)** Differential activation in response to the spoken words task in CI > controls highlights the group differences in certain brain areas. The first column shows unthresholded β maps and the second column shows t-statistic maps thresholded at voxelwise p < 0.05 (uncorrected) for each group.

250

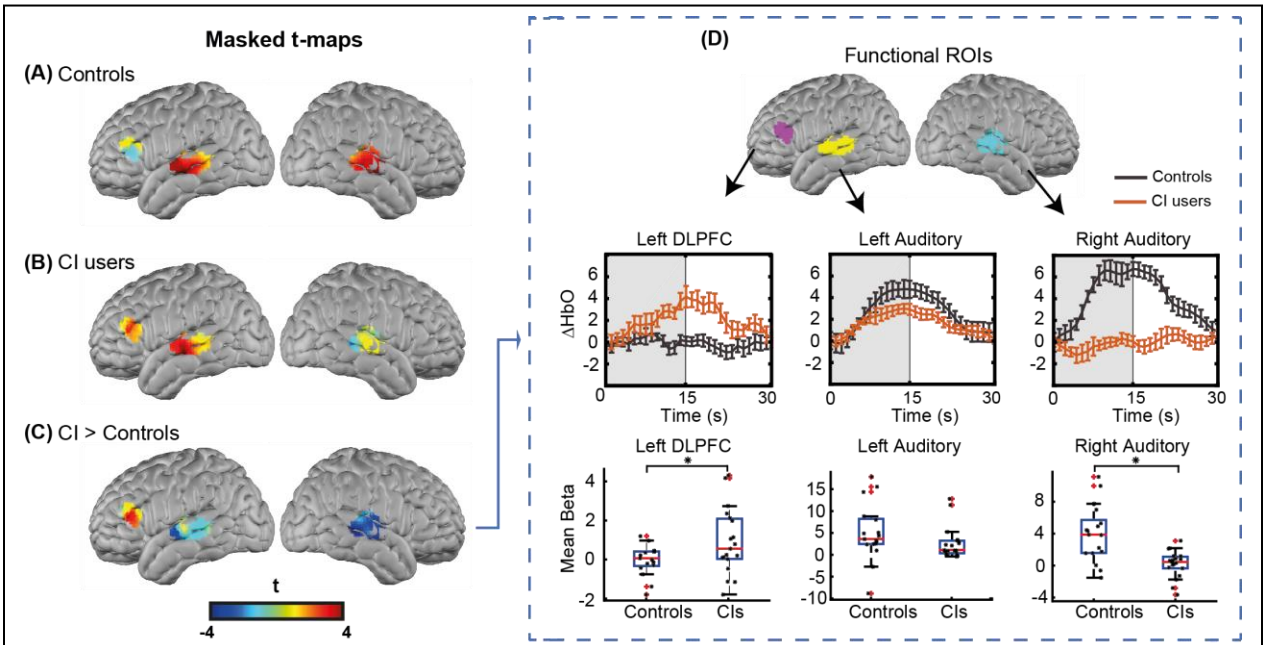

Figure 5 | ROI-based statistical analysis for spoken word recognition task. Unthresholded t-maps in response to the spoken words spatially masked in the three ROIs defined in **Fig. 3** in **(A)** 18 controls, **(B)** 20 right-ear CI users, and **(C)** CI > Controls, highlight the group differences in certain brain areas. **(D)** Temporal profile of the hemodynamic response in three selected ROIs (left DLPFC, left auditory, and right auditory cortices). Two-sample t-tests for mean β value in each ROI have been calculated between controls and the CI-user group, confirming a significant increase in left DLPFC in CI users and significant decrease in the right auditory cortex (depicted as a star (*) above their corresponding box plots).

Behavioral measures

An important consideration in studying CI users is the variability in their speech perception abilities, hearing thresholds, and the relationship with brain activity. **Figure 6** shows exploratory analyses between the magnitude of the activation in the left DLPFC ROI for the CI user cohort with respect to the speech perception score, left ear hearing threshold un-aided, left ear hearing threshold at test (aided if the subject used a hearing aid), and right ear hearing threshold (CI-aided).

Using $p < 0.05$ (uncorrected) as a statistical significance threshold, left DLPFC activation positively correlated with left ear unaided thresholds ($p = 0.01$) and negatively correlated with right ear CI-aided thresholds ($p = 0.02$). Left DLPFC activation did not correlate with speech perception score ($p = 0.4$) and aided hearing threshold for the left ear ($p = 0.1$).

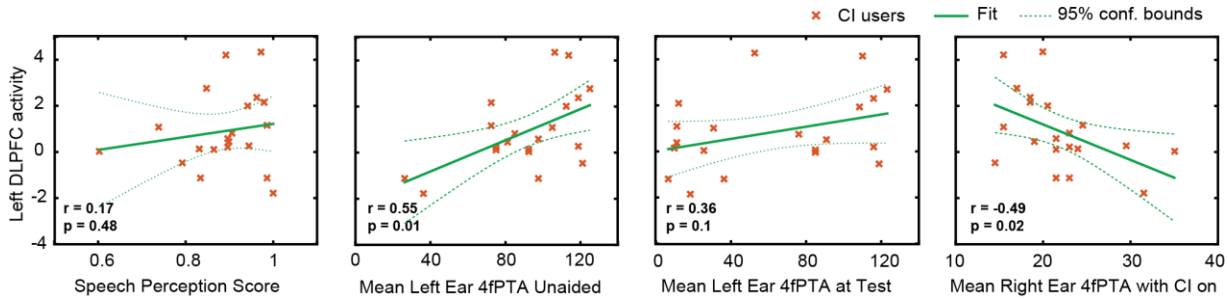

Figure 6 | Relationship between the magnitude of activation in left DLPFC and behavioral scores in CI users. Plots of the correlation between the magnitude of the mean β value in the left DLPFC ROI are shown with respect to speech perception score, left ear hearing threshold unaided, left ear hearing threshold (aided if the subject used a hearing aid), and right ear CI-aided hearing threshold. Hearing threshold was defined as 4fPTA, pure tone average at 4 frequencies, 500, 1000, 2000, 4000 Hz.

Discussion

Using high-density optical brain imaging, we examined the brain networks supporting spoken word recognition in listeners with CIs relative to a matched group of controls with bilateral normal hearing. We found that relative to controls, when listening to words, listeners with CIs showed reduced activity in the right auditory cortex and—critically—increased activity in left DLPFC. We review these two findings in turn below.

Reduced auditory cortical activity in CI users

We found reduced activity in the right auditory cortex in CI users relative to controls, which we attribute to differences in auditory stimulation. We limited our sample to CI listeners with unilateral right-sided implants but did not restrict left ear hearing. Most of our subjects with CIs had poor hearing in their left ears, which would result in reduced auditory information being passed to the contralateral (right) auditory cortex. This was as opposed to controls who had bilateral hearing. Prior fNIRS studies have also shown that activity in the superior temporal cortex corresponds with stimulation and comprehension (Olds, Pollonini et al. 2016, Zhou, Seghouane et al. 2018).

What is potentially more interesting is a lower level of activity in the left auditory cortex of the CI users compared to controls, even though all CI listeners were receiving adequate stimulation of their right auditory nerve with a right CI. There are several possible explanations for this finding. First, activity in superior temporal cortex does not reflect only “basic” auditory stimulation, but processing related to speech sounds, word meaning, and other levels of linguistic analysis. Thus, although subjects with CIs were certainly receiving stimulation and speech intelligibility scores were generally good, some variability was still present (mean speech perception score = 0.88, SD = 0.09). The overall level of speech processing was significantly ($p = 0.00005$) lower for CI users than controls (mean speech perception score = 0.99, SD = 0.01), resulting in decreased activity (indeed, because the depth of HD-DOT includes only about 1 cm of the brain, much of primary auditory cortex is not present in our field of view, and the observed group differences were localized in non-primary regions of STG and MTG).

Perhaps the most provocative explanation is that a reduction in top-down modulatory processes (Davis and Johnsrude 2007) plays out as reduced activity in the temporal cortex. That is, given that effortful listening depends on attention (Wild, Yusuf et al. 2012), it might be that

processes related to top-down prediction (Sohoglu, Peelle et al. 2012, Sohoglu, Peelle et al. 2014, Cope, Sohoglu et al. 2017) are muted when too much cognitive control is required for perceptual analysis. Reconciling this interpretation with predictive coding accounts of speech perception (Blank and Davis 2016, Sohoglu and Davis 2020) will require additional work.

Increased dorsolateral prefrontal cortex activity in CI users

When listening to spoken words in quiet, listeners with normal hearing typically engage the left and right superior temporal cortex, including primary and secondary auditory regions (Price, Wise et al. 1992, Binder, Frost et al. 2000, Wiggins, Anderson et al. 2016, Rogers, Jones et al. 2020). Our current results for controls show this same pattern. However, when listeners with CIs performed the same task, we found that they engaged left DLPFC significantly more than the controls.

Although we only tested a single level of speech difficulty (that is, speech in quiet), prior studies have parametrically varied speech intelligibility and found intelligibility-dependent responses in the prefrontal cortex. Use of several types of signal degradation (Davis and Johnsrude 2003), revealed a classic “inverted-U” shape response in the prefrontal cortex as a function of speech intelligibility, with activity increasing until the speech became very challenging and then tapering off. A similar pattern was reported in fNIRS (Lawrence, Wiggins et al. 2018).

A pervasive challenge for understanding the role of DLPFC in speech understanding is the close anatomical relationship of core language processing regions and domain-general regions of prefrontal cortex (Fedorenko et al. 2012). We attempted to add some degree of functional specificity to our interpretation by including a spatial working memory task presumed to strongly engage domain-general regions with minimal reliance on language processing (Duncan 2010, Alexandra, Jade et al. 2015). Ideally, we would have used functional ROIs individually created for each subject, however, we were not convinced that our data were sufficiently reliable at the single-subject level. Furthermore, we did not have spatial working memory task data for all subjects. Thus, our functional localization relies on group-average spatial working memory results should be interpreted with caution.

Individual differences in DLPFC activation during spoken word recognition

Because of the variability of outcomes in CI users (Firszt, Holden et al. 2004, Holden, Finley et al. 2013), one promising thought is that individual differences in brain activation may help explain variability in speech perception ability. Although our study was not powered for individual difference analysis (Yarkoni and Braver 2010), we conducted exploratory correlations to investigate this avenue of inquiry. Interestingly, we saw a trend such that poorer hearing in the left (non-CI) ear was correlated with increased activity in DLPFC. Our participants with CIs had significant variability in left ear hearing. Because the speech task was conducted using loudspeakers, we would expect both ears to contribute to accurate perception. Thus, poorer hearing in the left ear would create a greater acoustic challenge, with a correspondingly greater drain on cognitive resources. This interpretation will need additional data to be properly tested.

Conclusions

Using high-density optical neuroimaging, we found increased activity in DLPFC in listeners with cochlear implants compared to listeners with normal hearing. Our findings are consistent with a greater reliance on domain-general cognitive processing and provide a potential framework for the effort that many CI users need to expend during speech perception, even in quiet.

Acknowledgements

Research reported here was supported by grants R21DC015884, R21DC016086, R21MH109775, and K01MH103594 from the US National Institutes of Health. AS would like to thank helpful discussions with Abraham Z. Snyder, Andrew K. Fishell, Kalyan Tripathy, Karla M. Bergonzi, Zachary E. Markow, Mariel M. Schroeder, Monalisa Munsi, Emily Miller, Timothy Holden, and Sarah McConkey. We also want to thank our participants for their time and interest in our study.

Conflict of interest

The authors declare that the research was conducted in the absence of any commercial or financial relationships that could be construed as a potential conflict of interest.

References

A. T. Eggebrecht, J. P. C. (2019). from https://github.com/WUSTL-ORL/NeuroDOT_Beta.

Alexandra, W., J. Jade and D. John (2015). "How domain general is information coding in the brain? A meta-analysis of 93 multi-voxel pattern analysis studies." Frontiers in Human Neuroscience **9**.

Anderson, C. A., I. M. Wiggins, P. T. Kitterick and D. E. H. Hartley (2017). "Adaptive benefit of cross-modal plasticity following cochlear implantation in deaf adults." Proceedings of the National Academy of Sciences of the United States of America **114**(38): 10256-10261.

Binder, J. R., J. A. Frost, T. A. Hammeke, P. S. F. Bellgowan, J. A. Springer, J. N. Kaufman and E. T. Possing (2000). "Human temporal lobe activation by speech and nonspeech sounds." Cerebral Cortex **10**(5): 512-528.

Blank, H. and M. H. Davis (2016). "Prediction errors but not sharpened signals simulate multivoxel fMRI patterns during speech perception." PLoS biology **14**(11): e1002577.

Brainard, D. H. (1997). "The psychophysics toolbox." Spatial Vision **10**(4): 433-436.

Braver, T. S. (2012). "The variable nature of cognitive control: a dual mechanisms framework." Trends in Cognitive Sciences **16**(2): 106-113.

Cope, T. E., E. Sohoglu, W. Sedley, K. Patterson, P. S. Jones, J. Wiggins, C. Dawson, M. Grube, R. P. Carlyon, T. D. Griffiths, M. H. Davis and J. B. Rowe (2017). "Evidence for causal top-down frontal contributions to predictive processes in speech perception." Nature Communications **8**.

Cousins, K. A. Q., H. Dar, A. Wingfield and P. Miller (2014). "Acoustic masking disrupts time-dependent mechanisms of memory encoding in word-list recall." Memory & Cognition **42**(4): 622-638.

Davis, M. H. and I. S. Johnsrude (2003). "Hierarchical processing in spoken language comprehension." Journal of Neuroscience **23**(8): 3423-3431.

Davis, M. H. and I. S. Johnsrude (2007). "Hearing speech sounds: Top-down influences on the interface between audition and speech perception." Hearing Research **229**(1-2): 132-147.

Duncan, J. (2010). "The multiple-demand (MD) system of the primate brain: mental programs for intelligent behaviour." Trends in Cognitive Sciences **14**(4): 172-179.

Dwyer, N. Y., J. B. Firszt, R. M. J. E. Reeder and hearing (2014). "Effects of unilateral input and mode of hearing in the better ear: self-reported performance using the speech, spatial and qualities of hearing scale." **35**(1).

Eckert, M. A., V. Menon, A. Walczak, J. Ahlstrom, S. Denslow, A. Horwitz and J. R. Dubno (2009). "At the Heart of the Ventral Attention System: The Right Anterior Insula." Human Brain Mapping **30**(8): 2530-2541.

Eggebrecht, A. T., S. L. Ferradal, A. Robichaux-Viehoever, M. S. Hassanpour, H. Dehghani, A. Z. Snyder, T. Hershey and J. P. Culver (2014). "Mapping distributed brain function and networks with diffuse optical tomography." Nature Photonics **8**(6): 448-454.

Fedorenko, E., M. K. Behr and N. Kanwisher (2011). "Functional specificity for high-level linguistic processing in the human brain." Proceedings of the National Academy of Sciences of the United States of America **108**(39): 16428-16433.

Fedorenko, E., J. Duncan and N. Kanwisher (2012). "Language-Selective and Domain-General Regions Lie Side by Side within Broca's Area." Current Biology **22**(21): 2059-2062.

Fedorenko, E., J. Duncan and N. Kanwisher (2013). "Broad domain generality in focal regions of frontal and parietal cortex." Proceedings of the National Academy of Sciences of the United States of America **110**(41): 16616-16621.

Ferradal, S. L., A. T. Eggebrecht, M. Hassanpour, A. Z. Snyder and J. P. Culver (2014). "Atlas-based head modeling and spatial normalization for high-density diffuse optical tomography: In vivo validation against fMRI." Neuroimage **85**: 117-126.

Firszt, J. B., L. K. Holden, M. W. Skinner, E. A. Tobey, A. Peterson, W. Gaggl, C. L. Runge-Samuelson and P. A. Wackym (2004). "Recognition of speech presented at soft to loud levels by adult cochlear implant recipients of three cochlear implant systems." Ear and Hearing **25**(4): 375-387.

Fishell, A. K., T. M. Burns-Yocum, K. M. Bergonzi, A. T. Eggebrecht and J. P. Culver (2019). "Mapping brain function during naturalistic viewing using high-density diffuse optical tomography." Scientific Reports **9**.

Garcia, C., T. Goehring, S. Cosentino, R. E. Turner, J. M. Deeks, T. Brochier, T. Rughooputh, M. Bance and R. P. Carlyon (2021). "The Panoramic ECAP Method: Estimating Patient-Specific Patterns of Current Spread and Neural Health in Cochlear Implant Users." Jaro-Journal of the Association for Research in Otolaryngology.

Gregg, N. M., B. R. White, B. W. Zeff, A. J. Berger and J. P. Culver (2010). "Brain specificity of diffuse optical imaging: improvements from superficial signal regression and tomography." Frontiers in neuroenergetics **2**: 14.

Hassanpour, M. S., A. T. Eggebrecht, J. P. Culver and J. E. Peelle (2015). "Mapping cortical responses to speech using high-density diffuse optical tomography." Neuroimage **117**: 319-326.

Hassanpour, M. S., A. T. Eggebrecht, J. E. Peelle and J. P. Culver (2017). "Mapping effective connectivity within cortical networks with diffuse optical tomography." Neurophotonics **4**(4).

Hassanpour, M. S., B. R. White, A. T. Eggebrecht, S. L. Ferradal, A. Z. Snyder and J. P. Culver (2014). "Statistical analysis of high density diffuse optical tomography." Neuroimage **85**: 104-116.

Holden, L. K., C. C. Finley, J. B. Firszt, T. A. Holden, C. Brenner, L. G. Potts, B. D. Gotter, S. S. Vanderhoof, K. Mispagel, G. J. E. Heydebrand and hearing (2013). "Factors affecting open-set word recognition in adults with cochlear implants." **34**(3): 342.

Koeritzer, M. A., C. S. Rogers, K. J. Van Engen and J. E. Peelle (2018). "The Impact of Age, Background Noise, Semantic Ambiguity, and Hearing Loss on Recognition Memory for Spoken Sentences." Journal of Speech Language and Hearing Research **61**(3): 740-751.

Lawler, C. A., I. M. Wiggins, R. S. Dewey and D. E. Hartley (2015). "The use of functional near-infrared spectroscopy for measuring cortical reorganisation in cochlear implant users: A possible predictor of variable speech outcomes?" Cochlear implants international **16**(sup1): S30-S32.

Lawrence, R. J., I. M. Wiggins, C. A. Anderson, J. Davies-Thompson and D. E. H. Hartley (2018). "Cortical correlates of speech intelligibility measured using functional near-infrared spectroscopy (fNIRS)." Hearing Research **370**: 53-64.

Noyce, A. L., N. Cestero, S. W. Michalka, B. G. Shinn-Cunningham and D. C. Somers (2017). "Sensory-Biased and Multiple-Demand Processing in Human Lateral Frontal Cortex." Journal of Neuroscience **37**(36): 8755-8766.

436 Olds, C., L. Pollonini, H. Abaya, J. Larky, M. Loy, H. Bortfeld, M. S. Beauchamp and J. S.
437 Oghalai (2016). "Cortical Activation Patterns Correlate with Speech Understanding After
438 Cochlear Implantation." Ear and Hearing **37**(3): E160-E172.
439 Peelle, J. E. (2017). "Optical neuroimaging of spoken language." Language Cognition and
440 Neuroscience **32**(7): 847-854.
441 Peelle, J. E. (2018). "Listening Effort: How the Cognitive Consequences of Acoustic Challenge
442 Are Reflected in Brain and Behavior." Ear and Hearing **39**(2): 204-214.
443 Price, C., R. Wise, S. Ramsay, K. Friston, D. Howard, K. Patterson and R. Frackowiak (1992).
444 "Regional Response Differences within the Human Auditory-Cortex When Listening to Words."
445 Neuroscience Letters **146**(2): 179-182.
446 Rabbitt, P. M. A. (1968). "Channel-Capacity Intelligibility and Immediate Memory." Quarterly
447 Journal of Experimental Psychology **20**: 241-&.
448 Rogers, C. S., M. S. Jones, S. McConkey, B. Spehar, K. J. Van Engen, M. S. Sommers and J.
449 E. J. N. o. L. Peelle (2020). "Age-related differences in auditory cortex activity during spoken
450 word recognition." **1**(4): 452-473.
451 Schroeder, M. L., A. Sherafati, R. L. Ulbrich, A. K. Fishell, A. M. Svoboda, J. P. Culver and A. T.
452 Eggebrecht (2020). Mapping Cortical Activations Underlying Naturalistic Language Generation
453 Without Motion Censoring Using HD-DOT. Optical Tomography and Spectroscopy, Optical
454 Society of America.
455 Sherafati, A., A. Z. Snyder, A. T. Eggebrecht, K. M. Bergonzi, T. M. Burns-Yocum, H. M. Lugar,
456 S. L. Ferradal, A. Robichaux-Viehoever, C. D. Smyser, B. Palanca, T. Hershey and J. P. Culver
457 (2020). "Global motion detection and censoring in high-density diffuse optical tomography."
458 Human Brain Mapping **41**(14): 4093-4112.
459 Sohoglu, E. and M. H. Davis (2020). "Rapid computations of spectrotemporal prediction error
460 support perception of degraded speech." Elife **9**.
461 Sohoglu, E., J. E. Peelle, R. P. Carlyon and M. H. Davis (2012). "Predictive Top-Down
462 Integration of Prior Knowledge during Speech Perception." Journal of Neuroscience **32**(25):
463 8443-8453.
464 Sohoglu, E., J. E. Peelle, R. P. Carlyon and M. H. Davis (2014). "Top-Down Influences of
465 Written Text on Perceived Clarity of Degraded Speech." Journal of Experimental Psychology-
466 Human Perception and Performance **40**(1): 186-199.
467 Vaden, K. I., S. E. Kuchinsky, S. L. Cute, J. B. Ahlstrom, J. R. Dubno and M. A. Eckert (2013).
468 "The Cingulo-Opercular Network Provides Word-Recognition Benefit." Journal of Neuroscience
469 **33**(48): 18979-18986.
470 Vaden, K. I., S. Teubner-Rhodes, J. B. Ahlstrom, J. R. Dubno and M. A. Eckert (2017).
471 "Cingulo-opercular activity affects incidental memory encoding for speech in noise."
472 Neuroimage **157**: 381-387.
473 Ward, C. M., C. S. Rogers, K. J. Van Engen and J. E. Peelle (2016). "Effects of Age, Acoustic
474 Challenge, and Verbal Working Memory on Recall of Narrative Speech." Experimental Aging
475 Research **42**(1): 126-144.
476 White, B. R. and J. P. Culver (2010). "Quantitative evaluation of high-density diffuse optical
477 tomography: in vivo resolution and mapping performance." Journal of Biomedical Optics **15**(2).
478 Wiggins, I. M., C. A. Anderson, P. T. Kitterick and D. E. Hartley (2016). "Speech-evoked
479 activation in adult temporal cortex measured using functional near-infrared spectroscopy
480 (fNIRS): Are the measurements reliable?" Hear Res **339**: 142-154.
481 Wild, C. J., A. Yusuf, D. E. Wilson, J. E. Peelle, M. H. Davis and I. S. Johnsrude (2012).
482 "Effortful Listening: The Processing of Degraded Speech Depends Critically on Attention."
483 Journal of Neuroscience **32**(40): 14010-14021.
484 Wingfield, A. (2016). "Evolution of Models of Working Memory and Cognitive Resources." Ear
485 and Hearing **37**: 35s-43s.

Yarkoni, T. and T. S. Braver (2010). Cognitive neuroscience approaches to individual differences in working memory and executive control: conceptual and methodological issues. Handbook of individual differences in cognition, Springer**:** 87-107.

Zhou, X., A. Seghouane, A. Shah, H. Innes-Brown, W. Cross, R. Litovsky and C. M. McKay (2018). "Cortical Speech Processing in Postlingually Deaf Adult Cochlear Implant Users, as Revealed by Functional Near-Infrared Spectroscopy." Trends in Hearing **22**.